


Airflow driven fluid–structure interaction subjected to aqueous-based liquid spraying

Cite as: Phys. Fluids **32**, 081901 (2020); <https://doi.org/10.1063/5.0015587>

Submitted: 29 May 2020 . Accepted: 15 July 2020 . Published Online: 03 August 2020

A. Bouvet, X. Pelorson, and A. Van Hirtum 



View Online



Export Citation



CrossMark

ARTICLES YOU MAY BE INTERESTED IN

Passive and active control of turbulent flows

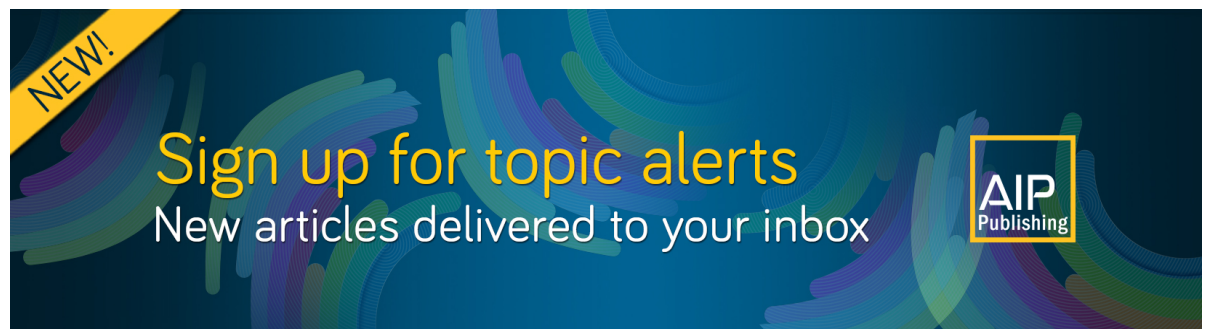
Physics of Fluids **32**, 080401 (2020); <https://doi.org/10.1063/5.0022548>

Pulsed-jet propulsion via shape deformation of an axisymmetric swimmer

Physics of Fluids **32**, 081902 (2020); <https://doi.org/10.1063/5.0015498>


Invisibility concentrator for water waves

Physics of Fluids **32**, 081701 (2020); <https://doi.org/10.1063/5.0019129>



NEW!

Sign up for topic alerts
New articles delivered to your inbox



Airflow driven fluid–structure interaction subjected to aqueous-based liquid spraying

Cite as: *Phys. Fluids* **32**, 081901 (2020); doi: [10.1063/5.0015587](https://doi.org/10.1063/5.0015587)

Submitted: 29 May 2020 • Accepted: 15 July 2020 •

Published Online: 3 August 2020



View Online



Export Citation



CrossMark

A. Bouvet,^{a)} X. Pelorson,^{b)} and A. Van Hirtum^{c)} 

AFFILIATIONS

LEGI, UMR CNRS 5519, Grenoble Alpes University, Grenoble, France

^{a)}Electronic mail: anne.bouvet@univ-grenoble-alpes.fr

^{b)}Electronic mail: xavier.pelorson@univ-grenoble-alpes.fr

^{c)}Author to whom correspondence should be addressed: annemie.vanhirtum@univ-grenoble-alpes.fr

ABSTRACT

Artificial saliva sprays are commonly used to remedy vocal folds surface hydration. Vocal folds surface hydration and its effect on their auto-oscillation are studied experimentally using artificial vocal folds. The airflow is used to excite the vocal folds into auto-oscillation after which the vocal folds surface is sprayed with a liquid. The validity of the findings described in a previous study [A. Bouvet, X. Pelorson, and A. Van Hirtum, “Influence of water spraying on an oscillating channel,” *J. Fluids Struct.* **93**, 102840 (2020)] concerning the effect of water spraying is further investigated. First, artificial saliva sprays (up to 5 ml) are sprayed instead of water. It is shown that this allows us to address the effect of increased dynamic viscosity (up to 8 times compared to water) as other artificial saliva properties affecting air–liquid mixing and surface wettability remain similar to water. Second, the Reynolds number in the dry stage is systematically increased (with 60%) for constant spraying volume ≥ 3 ml. Regardless of the sprayed liquid and Reynolds number, oscillation cycles are characterized by an increase in mean upstream pressure, cycle-to-cycle variability, and a decrease in oscillation frequency due period doubling. Increasing the dynamic viscosity tends to reduce the magnitude of these tendencies for spraying volumes smaller than 3 ml, indicating that viscous liquid–gas mixing affects the flow regime. Systematic Reynolds number variation shows that liquid spraying increases the oscillation onset threshold pressure and that the magnitude of general tendencies is reduced. The assessed conditions and features are pertinent to human voice production after hydration with an artificial saliva spray burst.

Published under license by AIP Publishing. <https://doi.org/10.1063/5.0015587>

I. INTRODUCTION

Voiced speech sound production occurs due to an airflow-driven fluid–structure (FS) instability between the airflow coming from the lungs and the surrounding deformable vocal folds (VFs) tissues. The surface of human VFs is hydrated with a liquid layer,^{1,2} and it is established that good surface hydration diminishes phonotraumatic lesions^{2,3} and benefits voice quality.^{4–8} Hydration affects the oscillation frequency and its spectral features as well as the vocal effort, determined by the oscillation amplitude and needed upstream lung pressure. In addition, the cycle-to-cycle perturbations of the oscillation period and the amplitude, expressed by the jitter and shimmer, respectively, are clinical voice quality parameters sensible to hydration. Consequently, the use of artificial saliva sprays to remedy VF surface hydration is widespread.^{9–11}

Whereas the physical principles underlying the FS instability are well studied,^{12–17} the potential role of VF’s surface hydration in the FS interaction is only marginally investigated. Recently, the effect of surface hydration following water spraying on a deformable auto-oscillating channel portion inserted in a rigid tube was studied experimentally.^{18,19} The setup consists of a mechanical deformable VF replica, concretely a pressurized latex tube (PLT) VF replica, mounted between two rigid uniform tubes representing the trachea (inferior end) and oral tract (superior end), as illustrated in Fig. 1. Auto-oscillation near the oscillation onset pressure threshold, i.e., the minimum upstream pressure required to sustain oscillation, was considered, and perturbation measures expressing voice quality in clinical studies^{5,7,8} were quantified on the oscillating upstream pressure gathered before and after water spraying.¹⁸ The volume of sprayed water was systematically varied between 1 ml up to 5 ml so that the applied volume range is pertinent to spray bursts, nebulizing

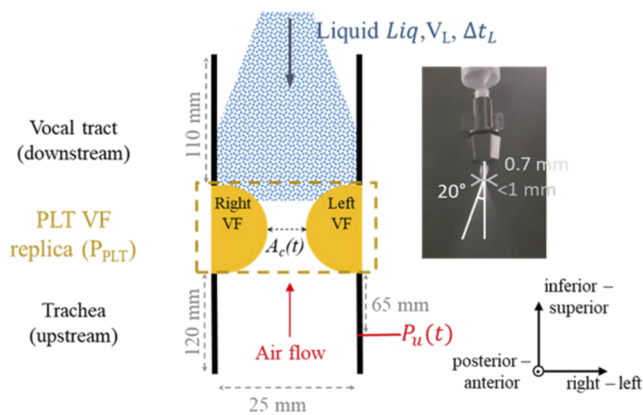


FIG. 1. Overview of the experimental setup: uniform rigid trachea pipe (upstream), uniform rigid vocal tract pipe (downstream), and in-between deformable mechanical PLT VF replica [elasticity condition P_{PLT} and glottal constriction area $A_c(t)$], liquid spray characteristics (label Liq , volume V_L , and spray duration Δt_L), and driving airflow [upstream pressure $P_u(t)$]. The sprayed liquid jet issuing from a syringe equipped with a spray nozzle is shown.

up to 4 ml each, during hydration remediation with artificial saliva sprays.¹⁰

The use of distilled water in previous studies^{18,19} was motivated by several reasons. From an experimental point of view, its fluid properties are well known, and it is readily available so that it provides a reference for other physical studies. This is particularly so since water spraying is applied in (de-)hydration studies involving human subjects^{1,7,8,10} and cadaver larynges.^{1,4,7} From a physiological point of view, water has similar density as reported for human saliva,^{9,20,21} and bi-directional water fluxes through the epithelium play an important role in regulating VF surface mucus hydration.^{1,22–24} Nevertheless, compared to human saliva, distilled water has a reduced dynamic viscosity. Therefore, the experiment and analysis described in Ref. 18 is first repeated for aqueous-based artificial saliva sprays in order to assess the effect of increased dynamic viscosity on the auto-oscillation.

In addition, previous experiments^{18,19} are re-assessed for upstream pressures near the oscillation onset threshold. Therefore, the experiment and analysis detailed in Ref. 18 are repeated for upstream driving pressures above the onset threshold in order to assess to which extent observations near the oscillation onset remain pertinent. In terms of human voice production, increasing the upstream or lung pressure corresponds to an increased vocal effort.

Both the upstream driving pressure and the dynamic viscosity of the spraying liquid might influence air–liquid fluid mixing. The fluid mixture determines the pressure distribution on the vocal folds walls within the glottal constriction.²⁵ Consequently, the fluid–structure interaction and the resulting auto-oscillation might be affected. The upstream pressure during oscillation is analyzed considering features commonly studied in vocal folds analysis.¹⁸

Consequently, the aim of this work is to consider the validity of the findings reported in Ref. 18 for water spraying, first, when an aqueous-based spraying liquid with increased dynamic viscosity is

used and, second, when the airflow pressure driving the FS interaction is increased above the one associated with the auto-oscillation onset.

II. SPRAYED LIQUID FLUID PROPERTIES

Three different spraying liquids are experimentally assessed in this work to mimic (re-)hydration: distilled water ($Liq0$) as in previous studies^{18,19} and two different aqueous-based liquids used in artificial saliva (AS) sprays, i.e., AS-Teijin ($Liq1$) and AS-Artisial ($Liq2$). The artificial sprays are commercially available in Japanese (for $Liq1$) and French (for $Liq2$) pharmacies, respectively. They are commonly used salines in order to remedy the lack of saliva by applying a burst of spray in the mouth (up to 4 ml). Both $Liq1$ and $Liq2$ are composed of different concentrations of sodium chloride, potassium chloride, and dipotassium phosphate. The liquid properties of interest (density ρ , dynamic viscosity μ , surface tension σ , contact angles, and pH) are determined at room temperature between 20 °C and 22 °C corresponding to temperatures for which experimental data are gathered. An overview is provided in Table I.

The density ρ is found as the ratio between the mass and volume. The volume is quantified using a micro-pipette with accuracy ± 0.1 ml, and its mass is obtained using a precision balance with accuracy ± 0.01 g. The tabulated ρ values are the averages of 10 repetitions.²⁶ The dynamic viscosity μ is obtained using a Cannon–Fenske viscometer with capillary diameters of 0.54 mm and 0.63 mm. The tabulated μ values indicate the averages of four repetitions.²⁶ The values for both artificial saliva sprays ($Liq1$ and $Liq2$) are compared with the values for distilled water ($Liq0$) and human saliva.^{9,20,21} Densities ρ for all assessed liquids ($Liq0$, $Liq1$, and $Liq2$) are approximately 1000 kg m^{-3} , similar to the values reported for human saliva. Compared to distilled water ($Liq0$, $\mu = 1 \text{ mPa s}$), dynamic viscosity μ is increased with approximately a factor of 5 for AS-Teijin ($Liq1$, $\mu = 4.95 \text{ mPa s}$) and a factor of 8 for AS-Artisial ($Liq2$, $\mu = 7.44 \text{ mPa s}$). It follows that whereas the viscosity of water is smaller than the range reported for human saliva, all assessed AS have μ -values within the range reported for human saliva. Note that the AS properties are similar to those in recent fluid studies involving saliva in the oral cavity.^{27,28}

The pendant drop method (drop generation with a syringe with diameter 1.7 mm, MotionBlitz EoSens Cube camera, macro-lens) is applied to determine the air–liquid surface tension σ using the Young–Laplace equation.²⁹ The values for AS ($Liq1$ and $Liq2$) are calculated to approximate $\sigma = 72 \text{ mN/m}$ characterizing water ($Liq0$). Note that $\sigma \approx 72 \text{ mN/m}$ obtained for all experimentally assessed liquids ($Liq0$, $Liq1$, and $Liq2$) is greater than the values reported for human saliva.^{9,21} For each liquid, the capillary length λ_c is then

TABLE I. Properties of spraying liquids ($Liq0$, $Liq1$, and $Liq2$) and human saliva.

	ρ (kg m^{-3})	μ (mPa s)	σ (mN/m)	λ_c (mm)	pH (-)
Saliva ^{9,20,21}	~ 1000	2.75-15.5	44-68	2.1-2.6	5.3-7.8
Water, $Liq0$	1000	1.00	72	2.7	6.80
AS-Teijin, $Liq1$	1014	4.95	71	2.7	8.04
AS-Artisial, $Liq2$	1015	7.44	72	2.7	6.72

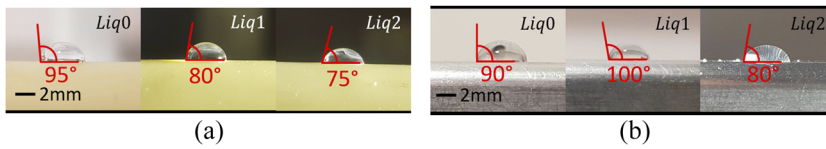


FIG. 2. Static contact angles θ_s measured for the experimentally assessed liquid droplets (water *Liq0*, AS-Teijin *Liq1*, and AS-Artisial *Liq2*) on the surfaces of (a) latex and (b) duralium.

obtained as

$$\lambda_c = \sqrt{\frac{\sigma}{\rho g}}, \tag{1}$$

with liquid density ρ and gravitational constant $g = 9.81 \text{ m/s}^{-2}$. The values are provided in Table I. As $\lambda_c = 2.7 \text{ mm}$ holds for all liquids, it is assumed that the sprayed liquid droplets are unaffected by gravity as $D_n < \lambda_c$ holds since the diameter $D_n \approx 0.7 \text{ mm}$, given the spray nozzle diameter as indicated in Fig. 1. It is noted that this approximates λ_c obtained for human saliva.

The wettability of the experimentally assessed spraying liquids (*Liq0*, *Liq1*, and *Liq2*) is assessed for latex and duralium surfaces. These surface materials are considered as they constitute the surfaces of the deformable (latex) and rigid (duralium) parts of the used experimental setup. The setup is schematically depicted in Fig. 1 and further detailed in Fig. 3. The static contact angles θ_s between the surface and a liquid droplet are shown in Fig. 2. All spraying liquids exhibit neutral wettability for these surface materials as static contact angles θ_s vary between 75° and 100° .^{30,31} Dynamic contact angles are measured for the least (water, *Liq0*) and the most viscous liquid (AS-Artisial, *Liq2*). The advancing θ_a and receding θ_r contact angles and their hysteresis $\theta_a - \theta_r$ are given in Table II. Similar values are obtained for both surfaces so that the values depend on the liquid. For both liquids, it is seen that the static contact angles θ_s approach the advancing contact angles θ_a to within 5° . The hysteresis doubles when comparing *Liq0* to *Liq2* as the receding contact angle is lowered. It is noted that the droplets used to test the wettability are smaller than the capillary length $\lambda_c = 2.7 \text{ mm}$ for all liquids as their diameter yields 1.7 mm .

For completeness, the measured pH values for spraying liquids (calibrated potentiometric pH/ORP meter Hanna Instr. HI2211, accuracy ± 0.01) are given in Table I. The values are within the upper range reported for human saliva.

As contact angles, capillary lengths, and surface tensions are similar for all experimentally assessed liquids, surface wetting and droplet deposition are assumed similar. It follows that the properties

of the experimentally assessed aqueous-based artificial saliva sprays AS-Teijin (*Liq1*) and AS-Artisial (*Liq2*) have similar properties as water, except for an increased dynamic viscosity μ . As such, these fluids allow us to study the influence of increased dynamic viscosity within the range pertinent to human saliva.

III. EXPERIMENTAL APPROACH

Auto-oscillation due to a fluid–structure interaction is generated by supplying airflow through a rigid channel (duralium, internal diameter 25 mm , neutral wettability) containing a deformable channel portion as a mechanical VF replica is inserted. The setup depicted in Fig. 1 is fully detailed in Ref. 18. Briefly, the deformable pressurized latex tube (PLT) VF replica (neutral wettability), illustrated in Fig. 3, consists of two pressurized latex tubes (thickness 0.2 mm , inferior–superior length $H = 12 \text{ mm}$, and posterior–anterior length $w = 25 \text{ mm}$) representing the left and right VF.^{18,26,32} These VF tubes are connected to a water column with a controllable height so that their internal pressure P_{PLT} , which determines its elasticity, can be varied. Both VFs are placed face to face in a metallic frame. The initial spacing between both VFs in the absence of airflow ranges from 30 mm^2 up to 70 mm^2 and results from the swelling of the latex tubes due to the imposed internal pressure P_{PLT} and from adjusting the micrometric screws. During VF auto-oscillation along the transverse right-left direction, the spacing between both VFs varies with time so that, in general, $A_c(t) \leq 100 \text{ mm}^2$ holds.³² A central latex tube (diameter 30 mm and thickness 0.2 mm) is placed between both VFs. This central latex tube is fixed to the upstream (streamwise length 11 cm , inferior of VFs) and downstream (streamwise length 12 cm , superior of VFs) channel portions representing the vocal tract and trachea, respectively, so that the airflow passes through without leakage. The replica is manually assembled so that the exact values depend on the montage (\mathcal{M}).

When airflow passes through the gap between both tubes, a fluid–structure interaction leads to auto-oscillation in the same way as during human phonation. Steady airflow (density $\rho_G = 1.2 \text{ kg m}^{-3}$, dynamic viscosity $\mu_G = 1.8 \times 10^{-5} \text{ Pa s}$, and temperature $22^\circ\text{C} \pm 2^\circ\text{C}$) is continuously provided to the flow channel along the streamwise inferior–superior direction by an air compressor (Atlas Copco GA5 FF-300-8, GA15 FF-8) connected to an upstream pressure reservoir (volume 0.22 m^3) filled with acoustic foam in order to avoid parasitic acoustic resonances and controlled with a valve (Norgren, 11-818-987). A pressure transducer (Endevco 8507C-5, accuracy $\pm 5 \text{ Pa}$) is positioned in a pressure tap situated 65 mm upstream of the VF replica in order to measure the upstream pressure $P_u(t)$. During experiments, the mean upstream pressure \bar{P}_u yields at least the auto-oscillation onset pressure P_{Onset} , which is the minimum upstream pressure required to sustain auto-oscillation for the VF replica in the dry configuration before liquid spraying.

TABLE II. Overview of contact angles for water (*Liq0*) and AS-Artisial (*Liq2*).

		Static	Dynamic		
			θ_s (deg)	θ_a (deg)	θ_r (deg)
Water, <i>Liq0</i>	Latex	95	98	77	21
	Duralium	90	94	72	22
AS-Artisial, <i>Liq2</i>	Latex	75	80	35	45
	Duralium	80	85	44	41

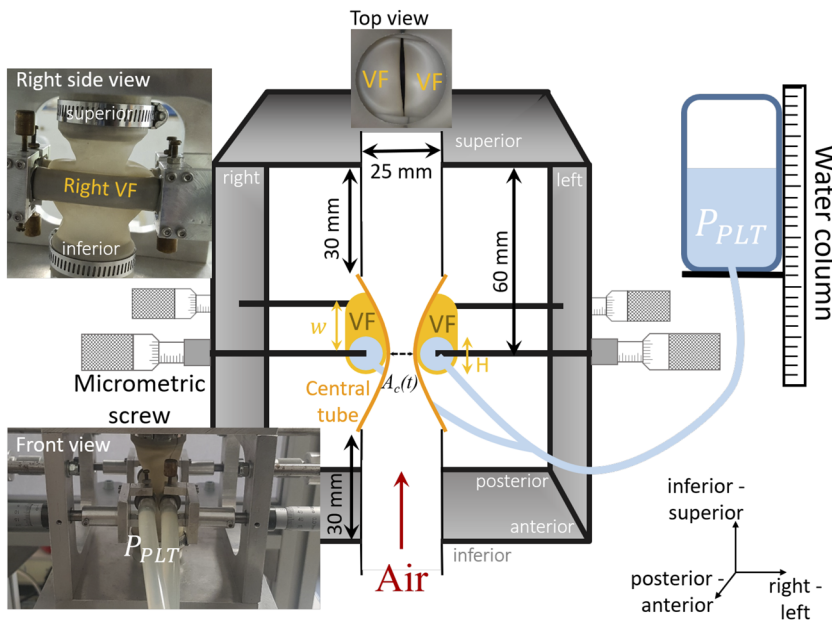


FIG. 3. Overview of the deformable pressurized latex tube (PLT) VF replica.

Liquid is sprayed at the downstream end of the flow channel, i.e., the downstream vocal tract outlet, in the superior–inferior direction, as depicted in Fig. 1.¹⁸ Note that this corresponds to the natural usage of AS sprays during which a spray burst is supplied through the mouth. Liquids discussed in Sec. II (*Liq0*, *Liq1*, or *Liq2*) are homogeneously sprayed by manually emptying a graduated syringe (accuracy 0.5 ml) with a known volume $V_L \leq 5$ ml. The syringe is equipped with a common spray nozzle (diameter $D_n = 0.7$ mm \pm 0.1 mm, length 10 mm, and diffusion angle 20°). During experiments, liquid spraying is time-tagged $t_L(t)$ by manually operating an electrical switch at the start and end of each spray burst so that its duration Δt_L corresponds to $t_L(t) > 0$. An overview of sprayed liquid volume V_L , spray duration Δt_L , liquid flow rate Φ_L , and jet bulk velocity at the nozzle exit U_L is given in Table III. Overall, liquid spraying has mean duration $\bar{\Delta t}_L = 1.62 \pm 0.6$ s, $\Delta t_L < 3$ s, mean liquid volume flow rate $\Phi_L = 1.75 \pm 0.40$ ml/s, and mean jet bulk velocity $\bar{U}_L = 4.55 \pm 1.02$ m/s.

The magnitudes and liquid properties given in Table I allow us to estimate the Weber number We ,

$$We = \frac{\rho U_L^2 D_n}{\sigma}, \quad (2)$$

and droplet relaxation time t_d ,

$$t_d = \frac{\rho D_n^2}{18\mu_G}, \quad (3)$$

for droplets with diameter D_n . For each of the assessed liquids (*Liq0*, *Liq1*, and *Liq2*), $We \approx 212 \pm 90$ and $t_d \approx 1.5$ s hold, which is the same magnitude as observed for human saliva (Table IV). Sprayed liquid jets are thus expected to break up into much smaller droplets as their diameter decreases, which favors mixing with the airflow. It follows that the Stokes number,

$$Stk = \frac{t_d U_G}{H}, \quad (4)$$

varies with U_G during the opening and closing phase of a single oscillation cycle, regardless of the assessed liquid. Mixing of the droplets with the airflow is expected when Stk is less than unity and surface hydration due to droplet deposition when Stk exceeds unity.

Temporal signals $P_u(t)$ and $t_L(t)$ are acquired (PC/DAQ, National Instruments PCI-MIO-16XE-10) with a sampling frequency of 10 kHz. The representative time traces of upstream pressure $P_u(t)$ and time tag $t_L(t)$ for a typical auto-oscillation experiment are shown in Fig. 4. During the first dry stage, 10 s steady-state

TABLE III. Overview of sprayed liquid volumes V_L , spray duration Δt_L , liquid volume flow rate Φ_L , and liquid jet bulk velocity U_L .

V_L (mL)	1	2	3	4	5
Δt_L (s)	0.82 ± 0.02	1.31 ± 0.08	1.70 ± 0.16	1.84 ± 0.18	2.41 ± 0.14
Φ_L (m ³ /s)	1.22×10^{-6}	1.52×10^{-6}	1.77×10^{-6}	2.18×10^{-6}	2.08×10^{-6}
U_L (m/s)	3.18	3.96	4.56	5.67	5.40

TABLE IV. Droplet properties for liquid spraying (*Liq0*, *Liq1*, and *Liq2*) and human saliva.

	$We (-)$					$t_d (s)$
	$V_L = 1 \text{ ml}$	$V_L = 2 \text{ ml}$	$V_L = 3 \text{ ml}$	$V_L = 4 \text{ ml}$	$V_L = 5 \text{ ml}$	$V_L \in [1 \text{ } 5] \text{ ml}$
Water, <i>Liq0</i>	98	152	202	313	284	1.51
AS-Teijin, <i>Liq1</i>	101	157	208	321	292	1.53
AS-Artisial, <i>Liq2</i>	100	155	205	317	288	1.53
Saliva ^{9,20,21}	100–500					1.51

auto-oscillation is gathered to characterize the dry configuration (subscript dry, $V_L = 0 \text{ ml}$). The second stage corresponds to liquid spraying characterized by the used liquid (*Liq0*, *Liq1*, or *Liq2*) and sprayed volume V_L . The third stage of 5 s, which yields about 3.3 times the droplet relaxation time t_d , allows stabilization after liquid spraying. The fourth liquid stage of 10 s is analyzed to study the effect of liquid spraying on the auto-oscillation established during the dry stage.

Mean upstream pressure \bar{P}_u during the dry stage (only airflow) provides an overestimation of the supplied airflow volume flow rate $Q_{\max,dry}$ as

$$Q_{\max,dry} = \sqrt{\frac{2\bar{P}_u}{\rho_G}} A_{c,\max} \cdot c_s, \quad (5)$$

with maximum constriction area $A_{c,\max} = 100 \text{ mm}^2$ and constant $c_s = 1.3$ accounting for flow detachment and jet formation along the diverging part of the glottal constriction.³³ An upper limit of THE Reynolds number Re_{dry} characterizing the dry stage is then obtained as

$$Re_{dry} = \frac{\rho_G Q_{\max,dry}}{\mu_G w}, \quad (6)$$

with posterior–anterior VF length $w = 25 \text{ mm}$, as depicted in Fig. 3. The Strouhal number Sr_{dry} of the oscillating flow during the dry stage is then estimated from the oscillation frequency f_0 as

$$Sr_{dry} = \frac{f_0 H}{Q_{\max,dry}} A_{c,\max} \cdot c_s, \quad (7)$$

with inferior–superior VF length $H = 12 \text{ mm}$, as indicated in Fig. 3.

In the dry stage ($V_L = 0 \text{ ml}$), both P_{Onset} and the associated oscillation frequency f_{Onset} depend on the imposed elasticity

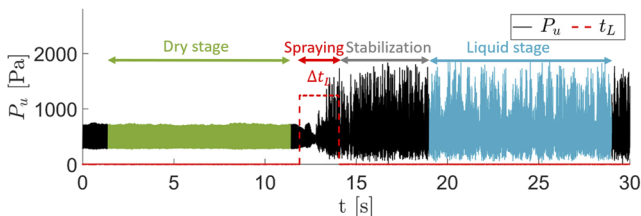


FIG. 4. Representative time traces of $P_u(t)$ and $t_L(t)$ indicating the consecutive stages: dry stage (10 s, $V_L = 0 \text{ ml}$), spraying stage (duration Δt_L , $V_L \leq 5 \text{ ml}$), 5 s stabilization, and liquid stage (10 s). The dry and liquid stages are analyzed.

condition P_{PLT} , as illustrated in Fig. 5. Upstream threshold pressures [Fig. 5(a)] at the auto-oscillation onset P_{Onset} and offset P_{Offset} exhibit a minimum due to changes in the initial glottal area and damping of mechanical resonances.¹² The minimum is obtained at $P_{PLT} \approx 3.3 \text{ kPa}$ for PLT VF replica montage *M I* [Fig. 5(a)]. The oscillation frequency f_{Onset} [Fig. 5(b)] increases quasi-linearly with P_{PLT} due to the increase in mechanical resonance frequencies $f_{1,2}^M$ measured from the frequency-response functions.^{18,26} The observed auto-oscillation threshold pressures $P_{Onset,Offset}$ and oscillation frequencies $f_{Onset,Offset}$ are within the range characterizing a normal human voice.^{34–36}

Liquid spraying is experimentally assessed for several elasticity conditions P_{PLT} , corresponding to vertical lines in Fig. 5, so that P_{Onset} and f_{Onset} characterizing the dry stage vary. In addition, the exact values vary as experiments are performed for two different PLT VF replica montages, labeled *M I* and *M II*.

The experimental conditions to study the influence of the dynamic viscosity of the sprayed liquid (liquid viscosity experiment) are summarized in Table V. For each spraying liquid (*Liq0*, *Liq1*, and

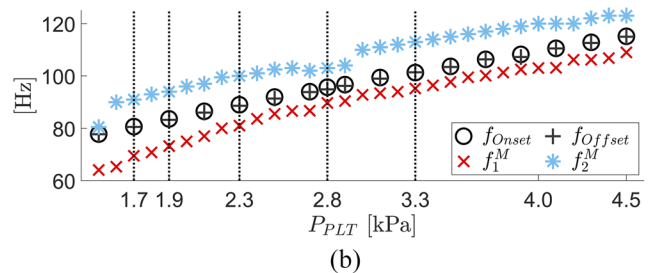
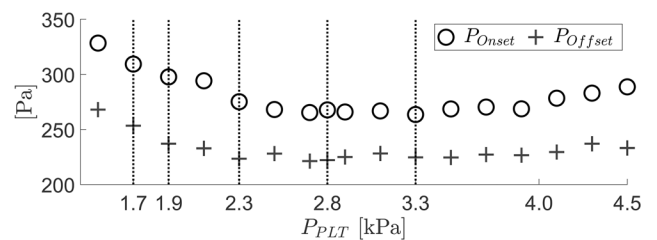


FIG. 5. Auto-oscillation onset (\circ) and offset ($+$) values as a function of elasticity condition P_{PLT} during the dry stage ($V_L = 0 \text{ ml}$) for PLT VF replica montage (*M I*): (a) upstream threshold pressures P_{Onset} and P_{Offset} and (b) oscillation frequencies f_{Onset} and f_{Offset} . Mechanical resonance frequencies f_1^M and f_2^M are given. Vertical lines indicate P_{PLT} for which the liquid is sprayed.

TABLE V. Overview of the liquid viscosity experiment.

\mathcal{M}	P_{PLT} (kPa)	Re_{dry}	Sr_{dry}	Liquid	V_L (mL)
I	2.8	8950	0.05	Liq0, Liq1, Liq2	(1–5)
I	3.3	7800	0.06	Liq0, Liq1, Liq2	(1–5)

TABLE VI. Overview of the airflow experiment.

\mathcal{M}	P_{PLT} (kPa)	Re_{dry}	Sr_{dry}	Liquid	V_L (ml)
II	1.7	5200-7500	0.11 – 0.078	Liq0	4
II	1.9	5200-7500	0.11 – 0.078	Liq0	4
II	2.3	5200-7500	0.11 – 0.078	Liq0	4
II	2.8	5200-7500	0.11 – 0.078	Liq0	4
I	3.3	7000-8300	0.060–0.023	Liq0, Liq2	3

Liq2), the sprayed volume V_L is varied. The experiment is repeated for two (P_{PLT} , Re_{dry})-combinations for PLT VF replica montage \mathcal{M} I.

Experimental conditions to study the influence of increasing the upstream driving pressure \bar{P}_u (airflow experiment) and hence Re_{dry} [Eq. (6)] during the dry phase are summarized in Table VI. For each assessed (P_{PLT} , V_L)-combination, Re_{dry} is increased from 5200 up to 7500 ($\approx 45\%$ Re_{dry} increase, Liq0, $V_L = 4$ ml, replica montage \mathcal{M} II) or from 7000 up to 8000 ($\approx 15\%$ Re_{dry} increase, Liq0 and Liq2, $V_L = 3$ ml, replica montage \mathcal{M} I).

For all experiments, $Sr_{dry} \leq 0.11$ holds and Re_{dry} is obtained by varying \bar{P}_u in the range of 120 Pa up to 400 Pa. The orders of magnitudes of Sr_{dry} and Re_{dry} are within the range associated with normal human voice production.^{34–36}

IV. UPSTREAM PRESSURE ANALYSIS

Ten second portions of upstream pressure $P_u(t)$ of the dry and liquid stages indicated in Fig. 4, corresponding to N_p oscillation cycles with $N_p > 400$, are analyzed. The mean oscillation characteristics and their fluctuations are objectively quantified following the approach detailed in Ref. 18. It is outlined in the Introduction that these features are assessed due to their use in clinical studies to express vocal effort and voice quality.^{2–8}

A cycle-to-cycle analysis is performed in order to retrieve the peak-to-peak amplitude \mathcal{A} and period T for each oscillation cycle from which their arithmetic means $\bar{\mathcal{A}}$ and \bar{T} are obtained. The cycle-to-cycle perturbations of amplitude $\zeta_{\mathcal{A}}$ and period ζ_T are obtained as

$$\zeta_{\mathcal{X}} = \frac{1}{N_p - 1} \frac{\sum_{i=1}^{N_p - 1} |\mathcal{X}_i - \mathcal{X}_{i+1}|}{\bar{\mathcal{X}}}, \quad (8)$$

with $\mathcal{X} = \mathcal{A}$ for the amplitude perturbations and $\mathcal{X} = T$ for the period perturbations. Note that, in voice quality studies, $\zeta_{\mathcal{A}}$ and ζ_T are labeled shimmer and jitter, respectively.

The overall harmonic content of $P_u(t)$ is quantified considering the total harmonic distortion rate THD and the signal-to-noise

ratio SNR . The THD compares the summed power of harmonic frequencies \mathcal{P}_{harm} with the power of the lowest harmonic frequency \mathcal{P}_{f_N} as

$$THD = 10 \log_{10} \left(\frac{\mathcal{P}_{harm}}{\mathcal{P}_{f_N}} \right). \quad (9)$$

The SNR compares the ratio of the summed power of all signal harmonics \mathcal{P}_{signal} to the summed power of the remaining noise \mathcal{P}_{noise} as

$$SNR = 10 \log_{10} \left(\frac{\mathcal{P}_{signal}}{\mathcal{P}_{noise}} \right). \quad (10)$$

Besides these general spectral features, the oscillation frequency f_N is quantified. As in Ref. 18, two oscillation frequencies are considered. First, $f_N \approx f_0$, where f_0 indicates the first harmonic frequency observed in the dry stage. Second, a quasi-subharmonic frequency $f_N \approx f_{0.5}$ due to period doubling in the liquid stage can appear so that $f_{0.5} \approx f_0/2$.^{18,19}

V. RESULTS

The features obtained for the liquid viscosity experiment (Sec. V A) and the airflow experiment (Sec. V B) are presented.

A. Liquid viscosity experiment

The experiments summarized in Table V for $V_L > 0$ ml allow us to compare the influence of spraying water (Liq0) with the influence of spraying artificial saliva sprays, AS-Teijin (Liq1) and AS-Artisial (Liq2). As a reference, the features obtained during the dry stage, i.e., without liquid spraying for $V_L = 0$ ml, are considered as well. The dynamic viscosity μ of water (Liq0) is increased by a factor of 4 using AS-Teijin (Liq1) and 8 using AS-Artisial (Liq2), as indicated in Table I. For each liquid, the features are plotted as a function of sprayed volume V_L . To avoid overlapping markers, the AS feature values are shifted around V_L .

The oscillation frequencies $f_N(V_L)$ for elasticity conditions $P_{PLT} \in \{2.8, 3.3\}$ kPa are plotted in Fig. 6. The first harmonic frequency f_0 is only marginally affected as liquid spraying results in a slight decrease ($<2\%$) from $f_0 \approx 102$ Hz characterizing $V_L = 0$ ml in accordance with Fig. 5(b). On the other hand, a near subharmonic frequency $f_{0.5}$ for $V_L \geq 1$ ml is generated associated with period doubling as previously observed for water spraying.^{18,19} The impact of dynamic viscosity on oscillation frequencies f_N is thus limited as same phenomena are observed, regardless of the sprayed liquid.

The mean upstream pressure \bar{P}_u (Fig. 7) and peak-to-peak cycle amplitude $\bar{\mathcal{A}}(V_L)$ (Fig. 8) show an overall increase. For all liquids, a transition occurs from the dry configuration for $V_L = 0$ ml up to a plateau reached in the range $V_L \geq 3$ ml. Within the plateau, \bar{P}_u augments with ≈ 100 Pa for both P_{PLT} , whereas the increase in $\bar{\mathcal{A}}$ depends on the elasticity and on the sprayed liquid. Although the liquid does not affect the general tendency, the increase tends to be limited or delayed with dynamic viscosity so that \bar{P}_u and $\bar{\mathcal{A}}(V_L)$ are smallest for Liq2 (AS-Artisial) within the transition region when $1 \leq V_L \leq 2$ ml. In the transition range, air-liquid mixing determines the flow behavior, whereas for $V_L \geq 3$ ml, liquid flow is expected to dominate the flow.²⁵ The found influence of dynamic viscosity is of particular interest for human voice production. The reduced

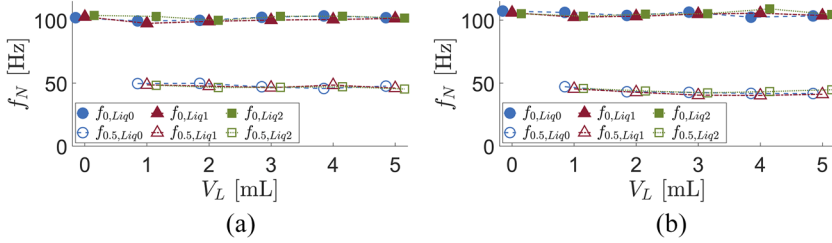


FIG. 6. Oscillation frequency $f_N(V_L)$ for all liquids (*Liq0*, *Liq1*, and *Liq2*) with the first harmonic $f_N = f_0$ (filled markers) or $f_N = f_{0.5}$ (empty markers): (a) $P_{PLT} = 2.8$ kPa and (b) $P_{PLT} = 3.3$ kPa.

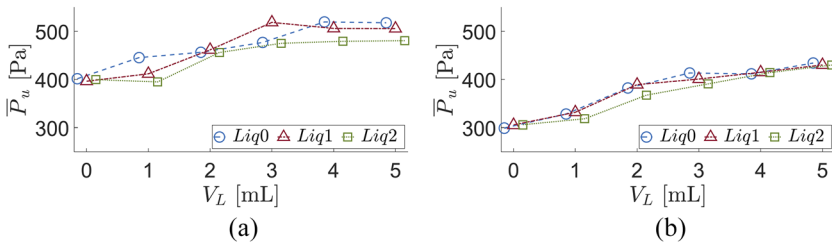


FIG. 7. Mean upstream pressure $\bar{P}_u(V_L)$ for all liquids (*Liq0*, *Liq1*, and *Liq2*): (a) $P_{PLT} = 2.8$ kPa and (b) $P_{PLT} = 3.3$ kPa.

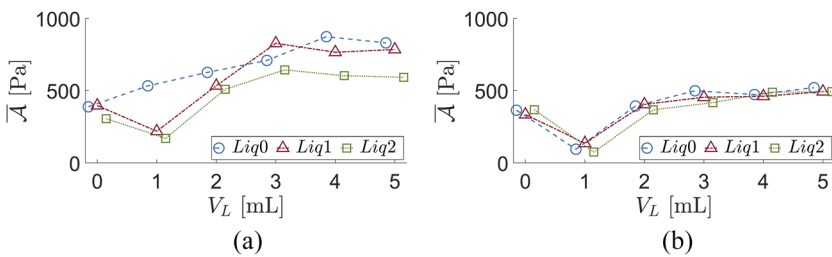


FIG. 8. Mean peak-to-peak cycle amplitude $\bar{A}(V_L)$ for all liquids (*Liq0*, *Liq1*, and *Liq2*): (a) $P_{PLT} = 2.8$ kPa and (b) $P_{PLT} = 3.3$ kPa.

upstream pressure \bar{P}_u and amplitude \bar{A} are considered beneficial for human voice as the auto-oscillation requires less effort and less impact. Furthermore, $\bar{A}(V_L)$ shows a minimum at $V_L = 1$ ml for *Liq1* and *Liq2* suggesting that an optimal voice condition exists, which, for the used replica, is reached for $V_L \approx 1$ ml. It is noted that these general tendencies do not hold at $P_{PLT} = 2.8$ kPa for *Liq1* at $V_L = 3$ ml as \bar{P}_u (Fig. 7) and $\bar{A}(V_L)$ (Fig. 8) are increased, with ≈ 35 Pa and ≈ 120 Pa, respectively, compared to the values obtained for *Liq0* at $V_L = 3$ ml. This is argued to be due to the influence of the liquid's viscosity on the liquid-air fluid mixing, which, in turn, determines the extent of the transition zone and hence the V_L associated with the plateau onset, which seems to shift to lower V_L as the liquid

viscosity increases. This mechanism remains to be detailed and confirmed in future research.

The cycle-to-cycle perturbation of the mean quantities discussed so far is considered. Note that the reduced cycle-to-cycle perturbation improves voice quality as well. The cycle-to-cycle perturbation curves of amplitude $\zeta_A(V_L)$ (Fig. 9) and period $\zeta_T(V_L)$ (Fig. 10) express that liquid spraying $V_L > 0$ ml introduces perturbation as $\zeta_{A,T} > 20\%$ holds compared to $\zeta_{A,T} < 4\%$ for $V_L = 0$ ml (dry). As for mean features \bar{P}_u and \bar{A} , the perturbation curves exhibit a transition zone for $0 < V_L < 3$ and a stable plateau zone for $V_L \geq 3$ ml. The perturbation degree is this large for all liquids due to period doubling associated with a loss of determinism described

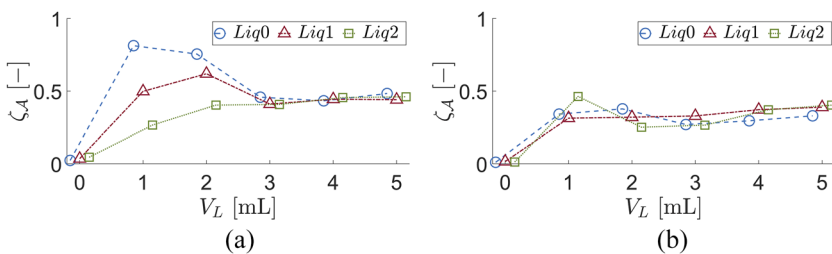


FIG. 9. Cycle-to-cycle amplitude perturbation $\zeta_A(V_L)$ for all liquids (*Liq0*, *Liq1*, and *Liq2*): (a) $P_{PLT} = 2.8$ kPa and (b) $P_{PLT} = 3.3$ kPa.

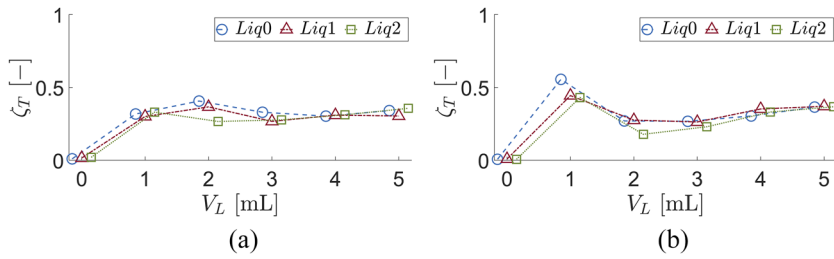


FIG. 10. Cycle-to-cycle period perturbation $\zeta_T(V_L)$ for all liquids (*Liq0*, *Liq1*, and *Liq2*): (a) $P_{PLT} = 2.8$ kPa and (b) $P_{PLT} = 3.3$ kPa.

for water spraying in Ref. 19. Nevertheless, as for mean \bar{P}_u and \bar{A} , increased viscosity provides again some regulation as it tends to limit the perturbation in the transition zone. The degree of perturbation decreases with liquid viscosity in the transition zone. This is most clearly observed considering $\zeta_A(V_L)$ (Fig. 9) for $P_{PLT} = 2.8$ kPa. As a maximum perturbation is found in the transition zone, it is of future interest to decrease the V_L -increment to refine the analysis in the transition zone. This is of particular interest considering elasticity conditions for which differences between liquids are less pronounced as is the case for $P_{PLT} = 3.3$ kPa. It is hypothesized that the different sensitivity to the liquid viscosity observed between elasticity conditions $P_{PLT} = 2.8$ kPa and $P_{PLT} = 3.3$ kPa is related to difference in stability of the auto-oscillation in the dry configuration. Supposing that a less stable auto-oscillation is more easily to be affected, it is suggested that the auto-oscillation at $V_L = 0$ ml is more stable for $P_{PLT} = 3.3$ kPa than for $P_{PLT} = 2.8$ kPa. Note that this is reasonable, given the increased Reynolds number needed for $P_{PLT} = 2.8$ kPa ($Re_{dry} = 8950$) compared to $P_{PLT} = 3.3$ kPa ($Re_{dry} = 7800$) (Table V).

The regulating capacity of dynamic viscosity μ in the transition zone for $0 < V_L < 3$ ml is also apparent considering the total harmonic distortion rate $THD(V_L)$ (Fig. 11) and signal-to-noise ratio $SNR(V_L)$ (Fig. 12) as the decrease in both THD and SNR reduces

with μ . It is noted that the imposed elasticity condition P_{PLT} affects the magnitude of observed tendencies as differences are again more pronounced for $P_{PLT} = 2.8$ kPa than for $P_{PLT} = 3.3$ kPa.

B. Airflow experiment

The influence of the airflow applied during the dry stage on the analysis stage is assessed from the experimental conditions summarized in Table VI. For each P_{PLT} condition, the features are plotted as a function of Re_{dry} defined in Eq. (6). For clarity, the values for different P_{PLT} are shifted around each Re_{dry} . In this section, each figure legend consists of multiple columns with three row entries. Each column corresponds to the same elasticity condition P_{PLT} indicated in the first row and represented in the figure by a unique symbol. The empty symbol in the second row entry corresponds to the dry condition $V_L = 0$ ml. The filled symbol in the third row entry corresponds to liquid spraying so that the imposed V_L or/and spraying liquid is indicated.

1. Influence of Re_{dry} : Water (*Liq0*)

First, the dry and liquid stages are analyzed for water (*Liq0*) spraying at $V_L = 4$ ml for PLT VF replica montage $\mathcal{M} II$ in Table VI. This is motivated from Sec. V A as features for water overlap with

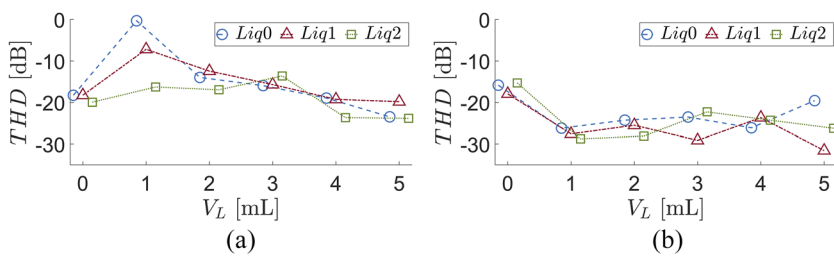


FIG. 11. Total harmonic distortion rate $THD(V_L)$ for all liquids (*Liq0*, *Liq1*, and *Liq2*): (a) $P_{PLT} = 2.8$ kPa and (b) $P_{PLT} = 3.3$ kPa.

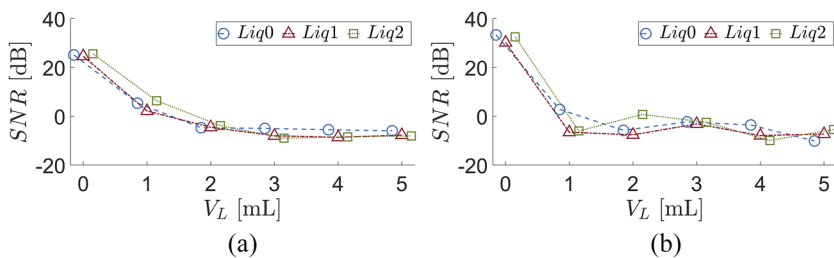


FIG. 12. Signal-to-noise ratio $SNR(V_L)$ for all liquids (*Liq0*, *Liq1*, and *Liq2*): (a) $P_{PLT} = 2.8$ kPa and (b) $P_{PLT} = 3.3$ kPa.

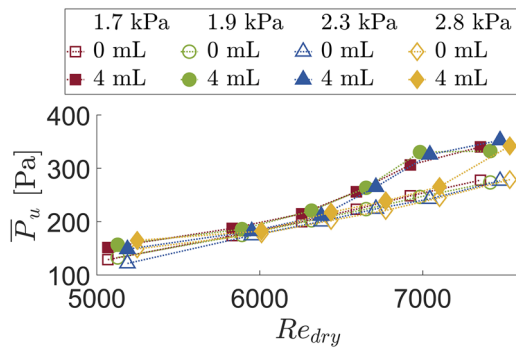


FIG. 13. Mean upstream pressure $\bar{P}_u(Re_{dry})$ for different P_{PLT} (kPa, symbols) in the dry (empty) and liquid (filled) stages for water (Liq0) spraying with $V_L = 4$ ml.

those obtained for AS for $V_L \geq 3$ ml. The mean upstream pressures \bar{P}_u are plotted in Fig. 13. For $Re_{dry} \approx 5200$, the imposed \bar{P}_u values in the dry stage are near the oscillation onset pressures so that $\bar{P}_u \approx P_{Onset}$, regardless of P_{PLT} . In general, the mean upstream pressures \bar{P}_u observed during the liquid stage are greater than the values observed during the dry stage. For $Re_{dry} \leq 6500$, the increase in \bar{P}_u with Re_{dry} observed during the liquid stage occurs at the same rate as the increase imposed during the dry stage for all elasticity conditions P_{PLT} . For $Re_{dry} > 6500$, the increase accelerates until it yields about 100 Pa. The increase is hypothesized to reflect the loss of stability and eventually the turbulent nature of the air–liquid fluid mixture for $Re_{dry} > 6500$, which needs to be further investigated in the future. The precise Re_{dry} at which \bar{P}_u starts to increase depends

on the elasticity condition P_{PLT} . The plotted curves in Fig. 13 suggest that increasing P_{PLT} delays the increase to larger Re_{dry} . This is expected from the decreasing onset pressure thresholds in this P_{PLT} -range [shown in Fig. 5(a)], suggesting that the oscillation stability increases with P_{PLT} so that higher Re_{dry} are needed to generate turbulence. It is noted that the increase in \bar{P}_u with 100 Pa between the dry ($V_L = 0$ ml) and liquid stages at $V_L = 4$ ml is consistent with the observations plotted in Fig. 7 for both $P_{PLT} = 2.8$ kPa ($Re_{dry} \approx 8950$ in Table V) and $P_{PLT} = 3.3$ kPa ($Re_{dry} \approx 7800$ in Table V).

The auto-oscillation frequencies $f_N(Re_{dry})$ are plotted in Fig. 14(a). For $\bar{P}_u \approx P_{Onset}$, water spraying causes the auto-oscillation to cease so that no features (filled symbols) are plotted for low Re_{dry} . In the dry stage, the oscillation frequency $f_N = f_0$ exhibits a small (less than 10%) decrease with Re_{dry} . In the liquid stage, a quasi-subharmonic frequency $f_N \approx f_{0.5}$ is observed, which shows a slight increase (less than 20%) with Re_{dry} . This is consistent with Fig. 6 and prior studies considering water spraying.^{18,19}

The mean cycle-to-cycle amplitudes $\bar{A}(Re_{dry})$ are presented in Fig. 14(b). The amplitude \bar{A} increases with Re_{dry} during both the dry and the liquid stage. Compared to the dry stage, the mean amplitudes are reduced in the liquid stage. Nevertheless, the increase slows down with Re_{dry} so that it is of interest to further extend the Re_{dry} range.

The presence of quasi-subharmonic frequency $f_{0.5}$ due to period doubling in the liquid stage indicates that complexity sets in when water is sprayed.¹⁹ The increased complexity is also apparent considering the increased cycle-to-cycle perturbation measures ζ_T and ζ_A plotted in Fig. 15. In the dry stage, both perturbation measures yield less than 5%, regardless of Re_{dry} . In the liquid stage, cycle-to-cycle irregularities result in a severe increase (>10%) of both

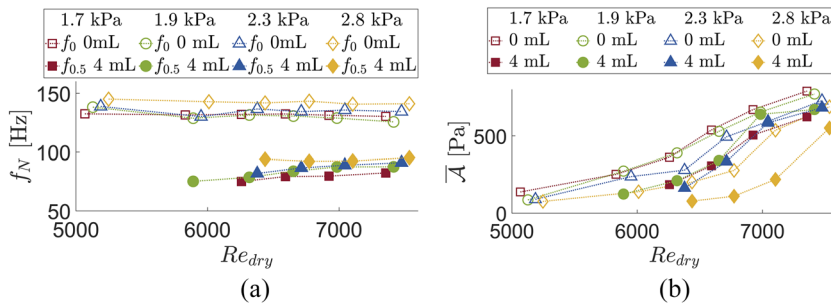


FIG. 14. Oscillation features for different P_{PLT} (kPa, symbols) in the dry (empty) and liquid (filled) stages for water (Liq0) spraying with $V_L = 4$ ml: (a) frequency $f_N(Re_{dry})$ and (b) peak-to-peak cycle amplitude $\bar{A}(Re_{dry})$.

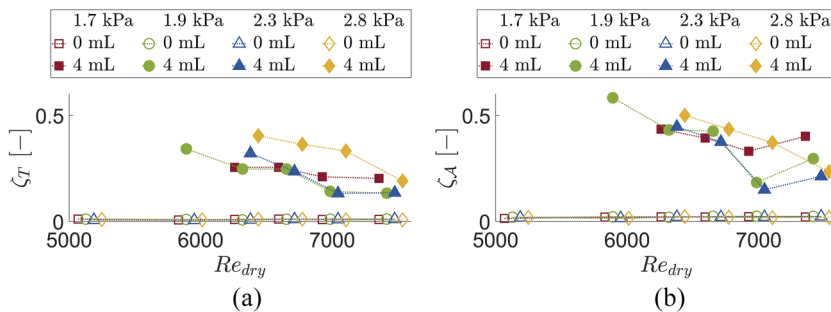


FIG. 15. Cycle-to-cycle perturbation features for different P_{PLT} (kPa, symbols) in the dry (empty) and liquid (filled) stages for $V_L = 4$ ml water (Liq0) spraying: (a) period $\zeta_T(Re_{dry})$ and (b) amplitude $\zeta_A(Re_{dry})$.

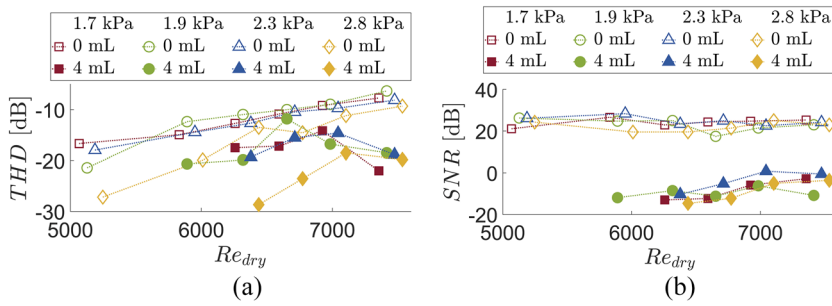


FIG. 16. Overall spectral features for different P_{PLT} (kPa, symbols) in the dry (empty) and liquid (filled) stages for $V_L = 4$ ml water (Liq0) spraying: (a) total harmonic distortion rate $THD(Re_{dry})$ and (b) signal-to-noise ratio $SNR(Re_{dry})$.

perturbation measures, which decrease with Re_{dry} . Considering again Figs. 13 and 14(b), this implies that the perturbation becomes less important as \bar{P}_u and therefore \bar{A} increases.

The overall spectral measures $THD(Re_{dry})$ and $SNR(Re_{dry})$ are plotted in Fig. 16. In the dry stage, THD increases with Re_{dry} (about 10 dB) for all elasticity conditions, whereas $SNR(Re_{dry})$ remains constant at about 25 dB. In the liquid stage, SNR [Fig. 16(b)] is reduced to 20 dB or more. The decrease is maximum for the lowest Re_{dry} for which auto-oscillation occurs and becomes less and less with Re_{dry} thereafter. This is in accordance with the tendencies observed for cycle-to-cycle perturbations $\zeta_{T,A}$. Therefore, in general, $\zeta_{T,A}$ and $SNR(Re_{dry})$ indicate that, in the liquid stage, increasing Re_{dry} stabilizes the auto-oscillation. From Fig. 16(a), it is seen that the overall

THD increases with Re_{dry} in both the dry and the liquid stage. Nevertheless, THD in the liquid stage is reduced compared to the dry stage.

2. Influence of Re_{dry} extended: Water (Liq0) and AS-Artisial (Liq2)

In this section, the auto-oscillation features for the experiment listed for PLT VF replica montage I in Table VI ($V_L = 3$ ml and $P_{PLT} = 3.3$ kPa) are quantified. This way, the impact of viscosity is further assessed using Liq0 and Liq2, while the findings for water spraying in the range $5200 \leq Re_{dry} \leq 7500$, addressed in Sec. V B 1 for Liq0 (montage M II), are extended to $5200 \leq Re_{dry} \leq 8300$. This is illustrated in Fig. 17 showing the mean upstream pressure $\bar{P}_u(Re_{dry})$

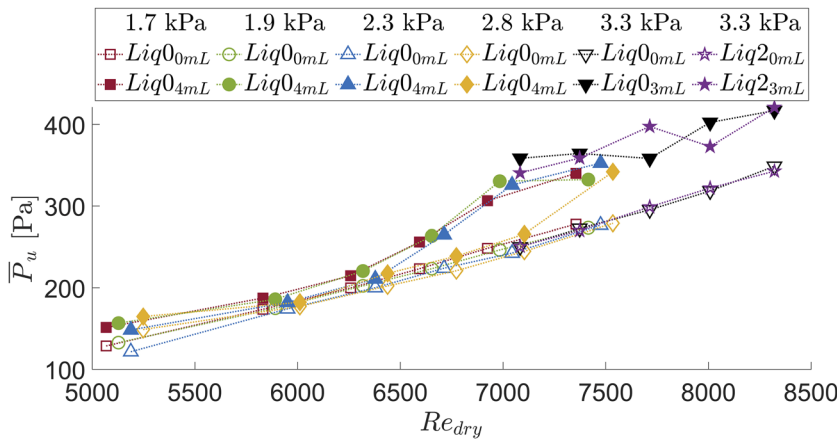


FIG. 17. Mean upstream pressure $\bar{P}_u(Re_{dry})$ for different P_{PLT} (kPa, symbols) in the dry (empty) and in the liquid (filled) stage for water (Liq0) and AS-artisial (Liq2) with $V_L \in \{3, 4\}$ ml (subscript).

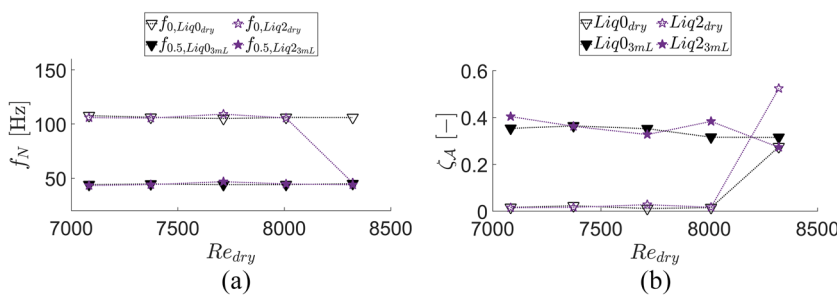


FIG. 18. Oscillation features for $P_{PLT} = 3.3$ kPa in the dry (empty) and in the liquid (filled) stage for water (Liq0, ∇) and AS-Artisial (Liq2, \star) with $V_L = 3$ ml: (a) frequency $f_N(Re_{dry})$ and (b) cycle-to-cycle amplitude perturbation $\zeta_A(Re_{dry})$.

for all flow experiments (montages $\mathcal{M} I$ and $\mathcal{M} II$) listed in Table VI. Overall, \bar{P}_u -tendencies observed for water ($Liq0$, $\mathcal{M} II$) up to $Re_{dry} \approx 7500$ keep on up to $Re_{dry} \approx 8300$ ($\mathcal{M} I$), regardless of the used liquid ($Liq0$ and $Liq2$). For each set of experiments (montages I and II), the maximum difference between the dry and the liquid stage remains of similar magnitude (≈ 100 Pa), regardless of the imposed elasticity condition P_{PLT} .

In general, the extracted features for $V_L = 3$ ml ($\mathcal{M} I$) confirm the findings described in Sec. V B 1 ($V_L = 4$ ml, montage $\mathcal{M} II$). This is illustrated in Fig. 18 for oscillation frequency $f_N(Re_{dry})$ and cycle-to-cycle amplitude perturbation $\zeta_A(Re_{dry})$. The oscillation frequency $f_N = f_0$ in the dry stage is reduced to $f_N \approx f_{0.5}$ in the liquid stage, whereas the cycle-to-cycle perturbation ζ_A increases from less than 5% in the dry stage to more than 20% in the liquid stage. Tendencies with Re_{dry} observed for other features (\bar{A} , ζ_T , SNR , and THD) also confirm the findings described in Sec. V B 1. It is noted that abnormal feature values in the dry stage are retrieved for $Re_{dry} = 8300$, e.g., f_N drops and ζ_A increases (Fig. 18). These abnormalities are due to f_0 sideband modulation caused by the central tube in the PLT VF replica (Fig. 3). As this is a limitation of the PLT VF replica, larger Re_{dry} values are not assessed.

VI. DISCUSSION AND CONCLUSION

Water and two commercially available artificial saliva sprays are sprayed (up to 5 ml) on an auto-oscillating channel mimicking vocal folds auto-oscillation. The used experimental protocol duplicates hydration with an artificial spray burst so that upstream pressure features without and after hydration are compared. It is seen that the liquid properties affecting air–liquid mixing and surface wettability are similar, except for the dynamic viscosity that is increased when artificial saliva sprays are used (up to 8 times).

In general, increasing the sprayed volume results in the increase in mean upstream pressure, cycle-to-cycle variability, and the decrease in oscillation frequency due period doubling. Therefore, general tendencies of quantified features confirm the previous observations for water spraying, and as such, general tendencies express the loss of determinism.^{18,19} Nevertheless, increasing the dynamic viscosity limits the magnitude of these tendencies for low spraying volumes up to 3 ml, providing further evidence that air–liquid mixing determines the flow regime in this case. This implies that hydration with an artificial spray instead of water can reduce the mean upstream pressure and oscillation amplitude, which benefits human voice production and reduces cycle-to-cycle perturbation that improves voice quality.

Liquid viscosity experiments were done at a constant Reynolds number. To consider the influence of upstream airflow supply on the fluid–structure interaction, the Reynolds number characterizing the dry stage is systematically increased from its value at the auto-oscillation onset threshold while the spraying volume is held constant at 3 ml or 4 ml. It is observed that, in the liquid stage, the oscillation onset threshold pressure is augmented compared to the dry stage. At the auto-oscillation onset, in the liquid stage, general tendencies associated with liquid spraying hold as cycle-to-cycle perturbation measures, mean upstream pressure, and signal-to-noise ratio increase, whereas the oscillation frequency reduces from f_0 to $f_{0.5}$. Further increasing the Reynolds number reduces the magnitude

of these tendencies for the assessed range of Reynolds numbers. It is verified that the used liquid does not affect these tendencies confirming that for spraying volumes ≥ 3 ml, the dynamic viscosity does not affect the observed features. It follows that increasing the airflow supply with respect to the auto-oscillation onset threshold might improve voice quality after hydration at the cost of a larger upstream pressure needed to sustain the auto-oscillation.

The discussed effects are studied for different PLT VF replica elasticity conditions P_{PLT} and montages \mathcal{M} . It is shown that the described tendencies remain although their magnitudes can be affected.

ACKNOWLEDGMENTS

The authors are grateful to Dr. I. Tokuda (Ritsumeikan Univ., Japan) and Tokyo Univ. Hospital for providing the artificial saliva spray AS-Teijin.

DATA AVAILABILITY

The data that support the findings of this study are available from the corresponding author upon reasonable request.

REFERENCES

- C. Leydon, M. Sivasankar, D. L. Falciglia, C. Atkins, and K. V. Fisher, "Vocal fold surface hydration: A review," *J. Voice* **23**, 658–665 (2009).
- J. Gartner-Schmidt, "Voice therapy for the treatment of voice disorders," in *Voice Therapy for the Treatment of Voice Disorders*, Head & Neck Surgery - Otolaryngology Vol. 1, 4th ed., edited by B. Bailey, J. Johnson, and S. Newlands (Lippincott Williams & Wilkins, Philadelphia, USA, 2006), p. 1388.
- K. Verdolini, I. R. Titze, and A. Fennell, "Dependence of phonatory effort on hydration level," *J. Speech, Lang., Hear. Res.* **37**, 1001–1007 (1994).
- S. Ayache, M. Ouaknine, P. H. Dejonkere, P. Prindere, and A. Giovanni, "Experimental study of the effects of surface mucus viscosity on the glottic cycle," *J. Voice* **18**, 107–115 (2004).
- C. Leydon, M. Wroblewski, N. Eichorn, and M. Sivasankar, "A meta-analysis of outcomes of hydration intervention on phonation threshold pressure," *J. Voice* **24**, 637–643 (2010).
- M. Dollinger, F. Grohn, D. Berry, U. Eysholdt, and G. Luegmair, "Preliminary results on the influence of engineered artificial mucus layer on phonation," *J. Speech, Lang., Hear. Res.* **57**, S637–S647 (2014).
- M. Alves, E. Kruger, B. Pillay, K. van Lierde, and J. van der Linde, "The effect of hydration on voice quality in adults: A systematic review," *J. Voice* **33**, 125.e13–125.e28 (2019).
- Z.-f. Zou, W. Chen, W. Li, and K. Yuan, "Impact of vocal fold dehydration on vocal function and its treatment," *Curr. Med. Sci.* **39**, 310–316 (2019).
- A. Yuan and R. Banerjee, "Comparison of artificial saliva substitutes," *Trends Biomater. Artif. Organs* **18**, 178–186 (2005).
- K. Tanner, N. Roy, R. M. Merrill, K. Kendall, K. L. Miller, D. O. Clegg, A. Heller, D. R. Houtz, and M. Elstad, "Comparing nebulized water versus saline after laryngeal desiccation challenge in Sjögren's syndrome," *Laryngoscope* **123**, 2787–2792 (2013).
- M. Sivasankar, T. Carroll, A. Kosinski, and C. Rosen, "Quantifying the effects of altering ambient humidity on ionic composition of vocal fold surface fluid," *Laryngoscope* **123**, 1275–1278 (2013).
- I. R. Titze, "The physics of small-amplitude oscillation of the vocal folds," *J. Acoust. Soc. Am.* **83**, 1536–1552 (1988).
- N. Rutu, X. Pelorson, A. Van Hirtum, I. Lopez-Arteaga, and A. Hirschberg, "An *in vitro* setup to test the relevance and the accuracy of low-order vocal folds models," *J. Acoust. Soc. Am.* **121**, 479–490 (2007).

- ¹⁴R. Mittal, B. D. Erath, and M. W. Plesniak, "Fluid dynamics of human phonation and speech," *Annu. Rev. Fluid Mech.* **45**, 437–467 (2013).
- ¹⁵J. Weili, Z. Xudong, and X. Qian, "Computational modeling of fluid-structure-acoustics interaction during voice production," *Front Bioeng. Biotechnol.* **5**, 7 (2017).
- ¹⁶A. Lodermeier, M. Tautz, S. Becker, M. Dollinger, V. Birk, and S. Kniesburges, "Aeroacoustic analysis of the human phonation process based on a hybrid acoustic PIV approach," *Exp. Fluids* **59**, 13 (2018).
- ¹⁷Z. Li, Y. Chen, S. Chang, and H. Luo, "A reduced-order flow model for fluid-structure interaction simulation of vocal fold vibration," *J. Biomech. Eng.* **142**, 021005 (2019).
- ¹⁸A. Bouvet, X. Pelorson, and A. Van Hirtum, "Influence of water spraying on an oscillating channel," *J. Fluids Struct.* **93**, 102840 (2020).
- ¹⁹A. Van Hirtum, A. Bouvet, and X. Pelorson, "Quantifying the auto-oscillation complexity following water spraying with interest for phonation," *Phys. Rev. E* **100**, 043111 (2019).
- ²⁰S. K. Lai, Y.-Y. Wang, D. Wirtz, and J. Hanes, "Micro- and macrorheology of mucus," *Adv. Drug Delivery Rev.* **61**, 86–100 (2009).
- ²¹S. Gittings, N. Turnbull, B. Henry, C. J. Roberts, and P. Gershkovich, "Characterisation of human saliva as a platform for oral dissolution medium development," *Eur. J. Pharm. Biopharm.* **91**, 16–24 (2015).
- ²²J. E. Phillips, L. B. Wong, and D. B. Yeates, "Bidirectional transepithelial water transport: Measurement and governing mechanisms," *Biophys. J.* **76**, 869–877 (1999).
- ²³K. V. Fisher, J. Ligon, J. L. Sobucks, and D. M. Roxe, "Phonatory effects of body fluid removal," *J. Speech, Lang., Hear. Res.* **44**, 354–367 (2001).
- ²⁴M. Sivasankar and K. V. Fisher, "Vocal fold epithelial response to luminal osmotic perturbation," *J. Speech, Lang., Hear. Res.* **50**, 886–898 (2007).
- ²⁵A. Van Hirtum, A. Bouvet, and X. Pelorson, "Pressure drop for adiabatic air-water flow through a time-varying constriction," *Phys. Fluids* **30**, 101901 (2018).
- ²⁶A. Bouvet, "Experimental and theoretical contribution to the analysis and the modelling of the vocal folds vibration," Ph.D. thesis, Grenoble Alpes University, France, 2019.
- ²⁷B. Scharfman, A. Techet, J. Bush, and L. Bourouiba, "Visualization of sneeze ejecta: Steps of fluid fragmentation leading to respiratory droplets," *Exp. Fluids* **57**, 24 (2016).
- ²⁸T. Dbouk and D. Drikakis, "On coughing and airborne droplet transmission to humans," *Phys. Fluids* **32**, 053310 (2020).
- ²⁹J. D. Berry, M. J. Neeson, R. R. Dagastine, D. Y. C. Chan, and R. F. Tabor, "Measurement of surface and interfacial tension using pendant drop tensiometry," *J. Colloid Interface Sci.* **454**, 226–237 (2015).
- ³⁰P. G. de Gennes, "Wetting: Statics and dynamics," *Rev. Mod. Phys.* **57**, 827–863 (1985).
- ³¹W. Abdallah, J. Buckley, A. Carnegie, J. Edwards, B. Herod, E. Fordham, A. Graue, T. Habashy, N. Seleznev, C. Signer, H. Hussain, B. Montaron, and M. Ziauddin, "Fundamentals of wettability," *Oilfield Rev.* **19**, 44–61 (2007).
- ³²A. Van Hirtum and X. Pelorson, "High-speed imaging to study an auto-oscillating vocal fold replica for different initial conditions," *Int. J. Appl. Mech.* **9**, 1750064 (2017).
- ³³J. Cisonni, A. Van Hirtum, X. Pelorson, and J. Willems, "Theoretical simulation and experimental validation of inverse quasi-one-dimensional steady and unsteady glottal flow models," *J. Acoust. Soc. Am.* **124**, 535–545 (2008).
- ³⁴R. L. Plant, G. L. Freed, and R. E. Plant, "Direct measurement of onset and offset phonation threshold pressure in normal subjects," *J. Acoust. Soc. Am.* **116**, 3640–3646 (2004).
- ³⁵M. Hirano and K. R. McCormick, in *Clinical Examination of Voice* (Acoustical Society of America, 1986), Vol. 80, pp. 1273.
- ³⁶M. Hirano, S. Kurita, and T. Nakashima, "Growth, Development and Aging of Human Vocal Folds," in *Vocal Fold Physiology: Contemporary Research and Clinical Issues* (College-Hill Press, 1983), pp. 22–43.